

The influence of metal oxide additives on the molecular structures of surface tungsten oxide species on alumina. II. In situ conditions

Marlene M. Ostromecki, Loyd J. Burcham, Israel E. Wachs *

Zettlemoyer Center for Surface Studies and Department of Chemical Engineering, Lehigh University, Bethlehem, PA 18015, USA

Received 25 June 1997; accepted 9 October 1997

Abstract

The dehydrated Raman spectra of unpromoted $\text{WO}_3/\text{Al}_2\text{O}_3$ indicate that the tungsten oxide surface species have the mono-oxo structure and are present as tetrahedrally coordinated monomers at low loadings and as a mixture of tetrahedrally and octahedrally coordinated surface polymers at high loadings. The effect of introducing secondary metal oxide additives to $\text{WO}_3/\text{Al}_2\text{O}_3$ catalysts, where tungsten oxide is present as a two-dimensional surface metal oxide overlayer, was investigated with in situ Raman spectroscopy under dehydrated conditions. The secondary metal oxide additives P_2O_5 , SnO_2 , Fe_2O_3 , NiO , ZnO , CoO , CeO_2 and MgO coordinate directly to the oxide support without significantly interacting with the surface tungsten oxide phase. The secondary metal oxide additives La_2O_3 , CaO , K_2O and Na_2O directly interact with surface tungsten oxide species to form both a surface mixed metal oxide complex and, for La_2O_3 and CaO , a crystalline tungstate compound. The noninteracting additives tend to be acidic (P_2O_5 and SnO_2) or mildly basic (Fe_2O_3 , NiO , ZnO , CoO , CeO_2 and MgO) and the interacting additives tend to be more basic (La_2O_3 , CaO , K_2O and Na_2O). © 1998 Elsevier Science B.V. All rights reserved.

Keywords: Tungsten oxide; Secondary metal oxide additives; In situ Raman spectroscopy

1. Introduction

Tungsten oxide supported on alumina, in the form of a two-dimensional surface metal oxide overlayer, is an important solid acid catalyst for hydrocracking and hydrotreating processes in the petroleum industry [1–6]. Commercially, however, these catalysts often contain other additives which exist as promoters, passivating

agents, poisons, or impurities. For example, the additives NiO , CoO and P_2O_5 act as promoters for $\text{WO}_3/\text{Al}_2\text{O}_3$ when used as hydrotreating catalysts [7]; Fe_2O_3 is usually deposited as a poison during petroleum processing and MgO , SnO_2 , La_2O_3 , CeO_2 and ZnO act as passivating agents that mitigate the effects of poisons [8–11]. Metal oxides such as K_2O , Na_2O and CaO may also be introduced inadvertently into the catalyst during preparation of the alumina or of the $\text{WO}_3/\text{Al}_2\text{O}_3$ catalyst [8–11].

Unfortunately, few studies have been conducted on the effect of such additives on the

* Corresponding author. Tel.: +1-610-7584539; fax: +1-610-7586555; e-mail: gd00@lehigh.edu

structure of the active surface tungsten oxide species, although much is known about single metal oxide catalysts on various supports (for $\text{WO}_3/\text{Al}_2\text{O}_3$, see Refs. [12–23]). It is not currently possible to predict, from information about single supported metal oxide catalysts, the molecular structures of the surface species of supported mixed metal oxide catalysts due to potential synergistic interactions between the deposited metal oxides on the catalyst surface. However, knowledge of the local molecular structures of these surface metal oxide species in supported mixed metal oxide catalysts is critical for the development of molecular structure–reactivity relationships, since the local structure of these catalysts are related to their catalytic properties during reaction [24–26].

Furthermore, it is important to determine this information under dehydrated conditions, which are closer to reaction conditions, since previous Raman spectroscopy studies have shown that these supported metal oxide catalysts change structure upon hydration in ambient environments [27]. The structures of hydrated $\text{WO}_3/\text{Al}_2\text{O}_3$ surface species are discussed in Part I of this series [28], in which the tungsten oxide surface species are seen to detach from the alumina support and dissolve in a thin film of water (~ 8 wt%) on the catalyst surface. The hydrated tungstate structures are then determined by the aqueous chemistry of tungsten oxide, where the tungsten oxide ions present in solution depend on the net pH at the point of zero charge (pzc) of the thin aqueous layer [27,28].

In the present study, the influence of the additives P_2O_5 , SnO_2 , Fe_2O_3 , NiO , ZnO , CeO_2 , CoO , La_2O_3 , CaO , MgO , K_2O and Na_2O upon the molecular structures of the surface tungsten oxide species of the $\text{WO}_3/\text{Al}_2\text{O}_3$ catalyst has been studied with Raman spectroscopy under in situ dehydrated conditions. Raman spectroscopy is a very useful technique for obtaining information about the molecular structures of the surface metal oxide species present in supported metal oxide catalysts because of its ability to

discriminate between different metal oxide molecular structures, in situ capabilities, ease of data acquisition and compatibility with many different transition metal oxide systems [24–26,29–32]. The choice of a high surface area alumina support for this study is ideal since it does not give rise to Raman active modes, making it possible to directly monitor the surface tungsten oxide species that do produce strong Raman signals [14,27].

2. Experimental

2.1. Sample preparation

The $\text{WO}_3/\text{Al}_2\text{O}_3$ catalysts studied were investigated as a function of surface coverage: 10% $\text{WO}_3/\text{Al}_2\text{O}_3$ (0.36 monolayer coverage or 1.44 W atoms/ nm^2), 15% $\text{WO}_3/\text{Al}_2\text{O}_3$ (0.54 monolayer coverage or 2.2 W atoms/ nm^2) and 25% $\text{WO}_3/\text{Al}_2\text{O}_3$ (0.9 monolayer coverage or 3.6 W atom/ nm^2). The secondary metal oxide/ $\text{WO}_3/\text{Al}_2\text{O}_3$ catalysts were also studied as a function of surface coverage: 0.7 monolayer-equivalent coverage (0.36 monolayer of tungsten oxide and 0.36 monolayer of secondary metal oxide), 1.1 monolayer-equivalents coverage (0.54 monolayer of tungsten oxide and 0.54 monolayer of secondary metal oxide) and 1.8 monolayer-equivalents coverage (0.9 monolayer of tungsten oxide and 0.9 monolayer of secondary metal oxide). Therefore, equivalent numbers of atoms of tungsten oxide and secondary metal oxide existed on the alumina support for each mixed metal oxide catalyst. Additional information about the precursors and preparation methods employed can be found in Ref. [28].

2.2. Raman studies

The catalyst wafer was contained in an environmental quartz cell with flowing oxygen, heated to 450°C for ~ 10 min and cooled for ~ 10 min at room temperature. This cell was

then introduced into the Raman spectrometer and the laser beam was focused on the stationary sample. The laser power at the stationary cell was maintained at 25–30 mW. The acquisition time per scan was 30 s and 25–50 scans were taken. The Raman spectra of the 1.8 monolayer-equivalents $\text{Fe}_2\text{O}_3/\text{WO}_3/\text{Al}_2\text{O}_3$ and $\text{CoO}/\text{WO}_3/\text{Al}_2\text{O}_3$ catalysts are not presented due to compound formation induced by the concentrated laser light of the spectrometer. Additional information about the Raman spectrometer used can be found in Ref. [28].

3. Results

3.1. Raman spectra of the dehydrated catalysts

3.1.1. $\text{WO}_3/\text{Al}_2\text{O}_3$ catalysts

The in situ Raman spectra of the dehydrated $\text{WO}_3/\text{Al}_2\text{O}_3$ catalysts as a function of surface tungsten oxide loading are presented in Fig. 1. The Raman band due to the symmetric stretch of the terminal $\text{W}=\text{O}$ bond within WO_4 and WO_6 surface tungsten oxide species [12,23] shifts to a higher wavenumber, from 1004 to 1017 cm^{-1} , with increasing tungsten oxide content. The Raman band at $\sim 300 \text{ cm}^{-1}$ is assigned to the bending mode of WO_4 and WO_6 surface tungsten oxide species [12,23]. The Raman bands at ~ 580 and $\sim 210 \text{ cm}^{-1}$ are assigned to the symmetric stretching and bending modes of the $\text{W}-\text{O}-\text{W}$ linkages of the surface polytungsten oxide species, respectively [12,23], and these bands increase in intensity with increasing tungsten oxide content. Thus, the surface tungsten oxide species on alumina become more distorted and polymerized with increasing surface coverage. Crystalline WO_3 particles (bands at 808, 714 and 276 cm^{-1} [14]) are not present in the Raman spectra because the surface tungsten oxide coverage is below monolayer coverage (monolayer coverage corresponds to $\sim 28\% \text{ WO}_3/\text{Al}_2\text{O}_3$ [28]).

The broad band at $\sim 880 \text{ cm}^{-1}$ has been assigned by Vuurman et al. [23] as the symmet-

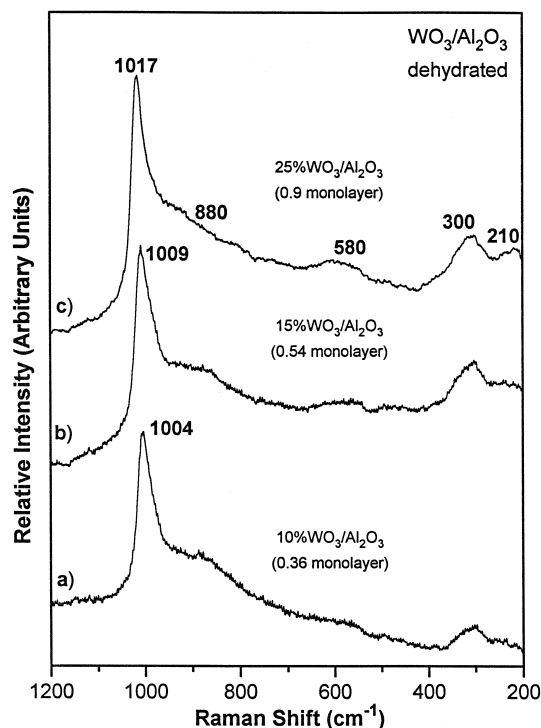


Fig. 1. (a) 10% $\text{WO}_3/\text{Al}_2\text{O}_3$ ($1.44 \text{ atom}/\text{nm}^2$), (b) 15% $\text{WO}_3/\text{Al}_2\text{O}_3$ ($2.2 \text{ atom}/\text{nm}^2$) and (c) 25% $\text{WO}_3/\text{Al}_2\text{O}_3$ ($3.6 \text{ atom}/\text{nm}^2$).

ric stretch of $\text{O}-\text{W}-\text{O}$ polymeric linkages and would be expected to increase more dramatically with increasing tungsten oxide loading than shown in Fig. 1 (since the other polymeric $\text{W}-\text{O}-\text{W}$ bands at ~ 580 and $\sim 210 \text{ cm}^{-1}$ increase with tungsten oxide loading). However, the broadness of this band is attributed, by Vuurman et al. [23], to a wide distribution of $\text{O}-\text{W}-\text{O}$ bond lengths. Furthermore, these authors have shown that under dehydrated conditions this band broadens and shifts upward as tungsten oxide loading is increased, most probably due to a further widening of the distribution of $\text{O}-\text{W}-\text{O}$ bond lengths. Thus, as loading is increased the $\sim 880 \text{ cm}^{-1}$ band appears to be less pronounced relative to the baseline, and instead appears as a very long and broad shoulder on the band attributed to the $\text{W}=\text{O}$ symmetric stretch (1017 cm^{-1}). Despite the broadening of the $\sim 880 \text{ cm}^{-1}$ band, an increase in the degree of polymerization with increased tung-

sten oxide loading is still clearly indicated by the increase in the W–O–W bands at ~ 580 and ~ 210 cm^{-1} . The structurally similar $\text{MoO}_3/\text{Al}_2\text{O}_3$ system further supports this interpretation, since the ~ 880 cm^{-1} band in this system does not broaden and shift, but rather it simply increases in intensity with loading (most likely due to a narrow distribution of O–Mo–O bond lengths) [23].

3.1.2. Secondary metal oxide / $\text{WO}_3/\text{Al}_2\text{O}_3$ catalysts

The Raman spectra of the promoted $\text{WO}_3/\text{Al}_2\text{O}_3$ samples under dehydration (Figs. 2–13) indicate that the secondary metal oxides studied may be grouped into two categories, those which have little or no interaction with the surface tungsten oxide species and those which interact strongly with the surface tungsten oxide species. Note that the Raman spectra are primar-

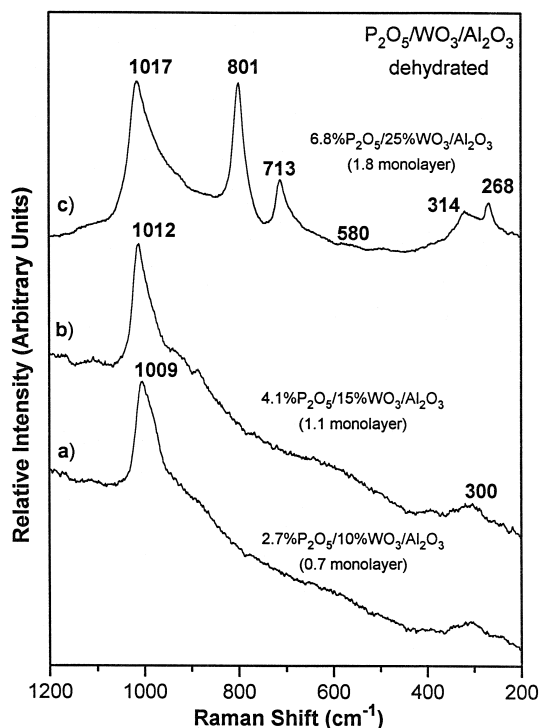


Fig. 2. (a) 2.7% $\text{P}_2\text{O}_5/10\%$ $\text{WO}_3/\text{Al}_2\text{O}_3$ (0.7 monolayer), (b) 4.1% $\text{P}_2\text{O}_5/15\%$ $\text{WO}_3/\text{Al}_2\text{O}_3$ (1.1 monolayer) and (c) 6.8% $\text{P}_2\text{O}_5/25\%$ $\text{WO}_3/\text{Al}_2\text{O}_3$ (1.8 monolayer).

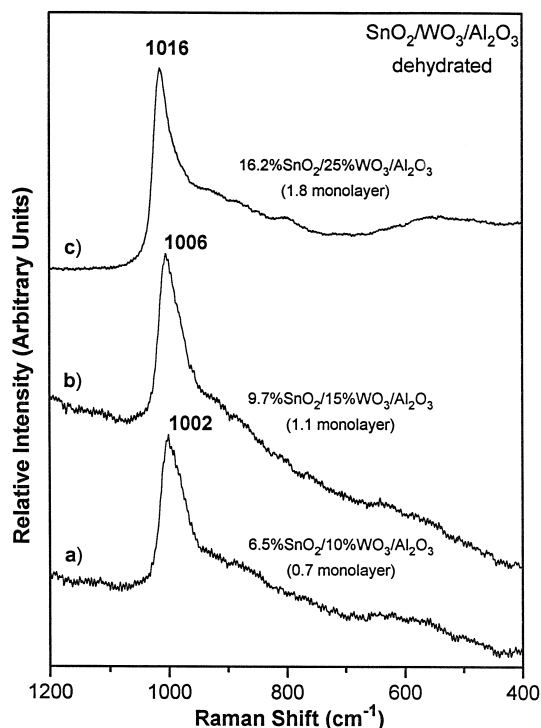


Fig. 3. (a) 6.5% $\text{SnO}_2/10\%$ $\text{WO}_3/\text{Al}_2\text{O}_3$ (0.7 monolayer), (b) 9.7% $\text{SnO}_2/15\%$ $\text{WO}_3/\text{Al}_2\text{O}_3$ (1.1 monolayer) and (c) 16% $\text{SnO}_2/25\%$ $\text{WO}_3/\text{Al}_2\text{O}_3$ (1.8 monolayer).

ily dominated by the tungsten oxide vibrational modes because the secondary metal oxide surface species have much weaker Raman scattering cross-sections than those of tungsten–oxygen bonds [14,33]. The Raman spectra of the promoted samples, therefore, provide direct information on the tungsten oxide surface species, but only limited information about the secondary metal oxides through their effect on the tungsten oxide surface species (e.g. shifts in the W=O band position and formation of crystalline compounds). Furthermore, the W=O symmetric stretching mode is generally the most frequency-sensitive Raman band to changes in the molecular structures of surface tungsten oxide species due to its sharpness and intensity. However, changes in the other bands at ~ 880 , ~ 580 , ~ 330 and ~ 210 cm^{-1} will be discussed in cases where they are significantly different from the unpromoted $\text{WO}_3/\text{Al}_2\text{O}_3$.

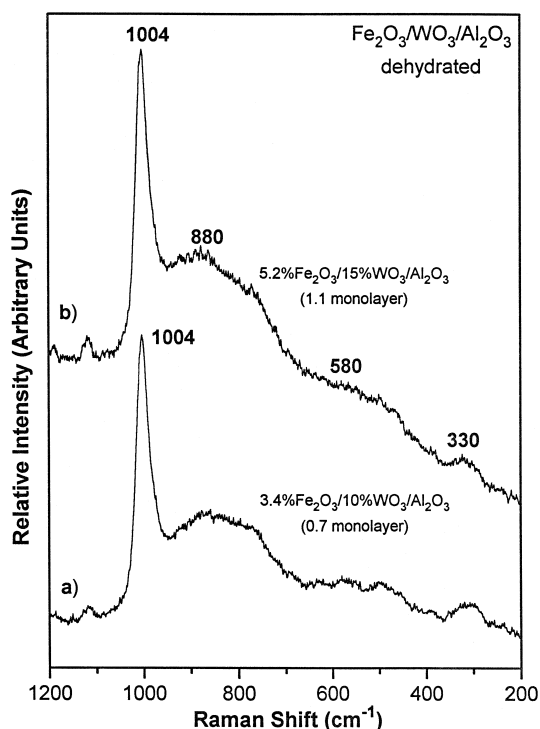


Fig. 4. (a) 3.4% Fe_2O_3 /10% WO_3 / Al_2O_3 (0.7 monolayer) and (b) 5.2% Fe_2O_3 /15% WO_3 / Al_2O_3 (1.1 monolayer).

The noninteracting secondary metal oxides include P_2O_5 , SnO_2 , Fe_2O_3 , NiO , ZnO , CoO , CeO_2 and MgO (Figs. 2–8 and 11, respectively). For these systems, the Raman frequencies of the $\text{W}=\text{O}$ symmetric stretching vibration are very similar to those of the original, unpromoted WO_3 / Al_2O_3 catalysts. Of course, care must be taken to compare the promoted catalysts at a given weight percent of WO_3 to the corresponding unpromoted WO_3 / Al_2O_3 catalysts with the same loading. Under this consideration, the variations in the frequencies of the $\text{W}=\text{O}$ symmetric stretch are only less than 8 cm^{-1} for nearly all of the loadings of these noninteracting catalysts and this is just outside the experimental frequency calibration error of $\pm 2\text{ cm}^{-1}$.

Among the noninteracting additives, only the highest loadings (1.8 monolayer-equivalents) of CeO_2 - and MgO -promoted catalysts display a slightly larger downshift in this $\text{W}=\text{O}$ vibration by 15 and 13 cm^{-1} , respectively. However,

because in the lower loadings of the ceria and magnesia promoted catalysts this band is within 5 cm^{-1} of its unpromoted values, CeO_2 and MgO may be considered generally noninteracting. Similarly, for Fe_2O_3 - and CoO -promoted catalysts at the highest loading (1.8 monolayer-equivalents), it is possible that Fe_2O_3 and CoO shift the $\text{W}=\text{O}$ symmetric stretching band down by amounts comparable to those observed for CeO_2 and MgO , since laser-induced compound formation prevented accurate measurement of these catalysts (note that the 1.8 monolayer-equivalents loading has been omitted in Figs. 4 and 7 and also note that under the present, dehydrated conditions the formations of iron and cobalt tungstate compounds at this loading are known to be induced by localized heating from the intense laser excitation source because under hydrated conditions [28] these catalysts do not exhibit Raman bands due to crystalline

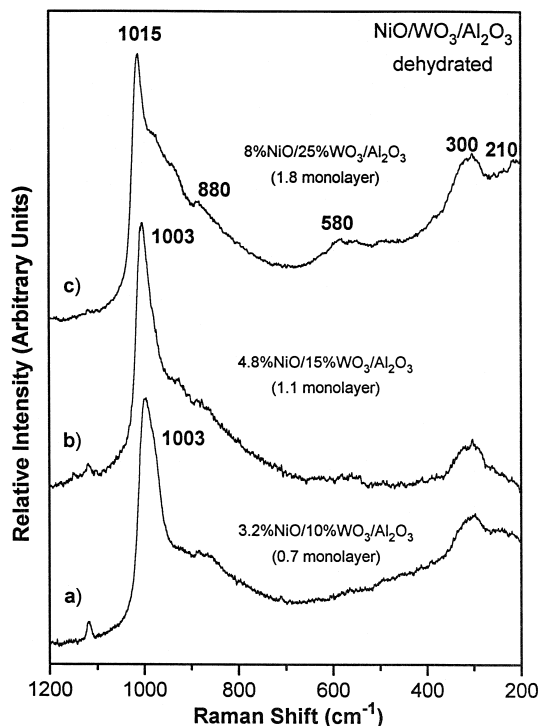


Fig. 5. (a) 3.2% NiO /10% WO_3 / Al_2O_3 (0.7 monolayer), (b) 4.8% NiO /15% WO_3 / Al_2O_3 (1.1 monolayer) and (c) 8% NiO /25% WO_3 / Al_2O_3 (1.8 monolayer).

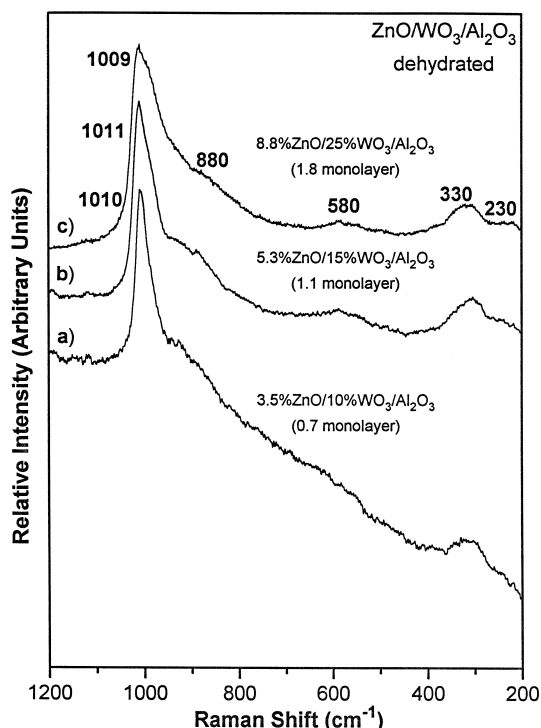


Fig. 6. (a) 3.5% ZnO/10% WO₃/Al₂O₃ (0.7 monolayer), (b) 5.3% ZnO/15% WO₃/Al₂O₃ (1.1 monolayer) and (c) 8.8% ZnO/25% WO₃/Al₂O₃ (1.8 monolayer).

compounds, which they would if compound formation occurred inherently during catalyst calcination). Again, however, in the lower loadings of the iron and cobalt oxide promoted catalysts the W=O symmetric stretching mode vibrates within 5 cm⁻¹ of its unpromoted values, so Fe₂O₃ and CoO may be considered generally noninteracting.

Minor exceptions among the noninteracting additives may include some very weak interaction with surface tungsten oxide and Fe₂O₃, NiO and CoO based on the fact that the ~ 880 cm⁻¹ band is qualitatively slightly more pronounced for these catalysts (Figs. 4, 5 and 7, respectively) than in unpromoted WO₃/Al₂O₃ (Fig. 1). Other minor exceptions include the presence of a small amount of WO₃ crystals (bands at 808, 714 and 276 cm⁻¹ [14]) for the Fe₂O₃-promoted catalysts and for the highest loading of the P₂O₅-promoted catalyst; as well

as an intense, sharp band at 457 cm⁻¹ in the ceria-promoted samples due to poorly dispersed CeO₂ crystals [34]. However, these weak Raman bands due to oxide microcrystallites must correspond to very small quantities of oxide crystals relative to surface tungsten oxide species, since the relative Raman scattering cross-section is much higher for oxide crystals than for surface species [14,33]. Finally, for the highest loading of the ceria-promoted catalyst the band at 944 cm⁻¹ may be due to very small amounts of a crystalline tungstate compound, possibly Ce₂(WO₄)₃ (Raman bands at 944, 925, 818, 727, 386 and 336 cm⁻¹ [35]), since the Raman band due to the symmetric stretch of O–W–O linkages does not have such a high frequency or intensity in pure 25% WO₃/Al₂O₃ (see Fig. 1c). A similar peak at 944 cm⁻¹ in the hydrated spectrum would confirm compound formation, but unfortunately the band for the W=O symmetric stretch in the surface tungsten

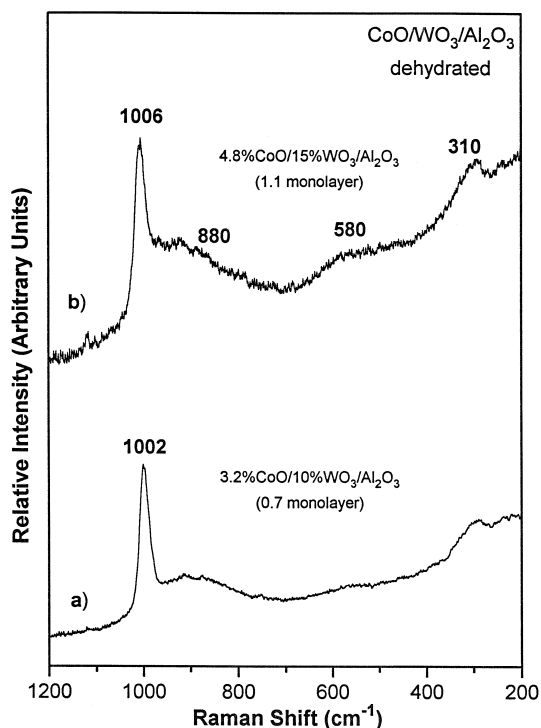


Fig. 7. (a) 3.2% CoO/10% WO₃/Al₂O₃ (0.7 monolayer) and (b) 4.8% CoO/15% WO₃/Al₂O₃ (1.1 monolayer).

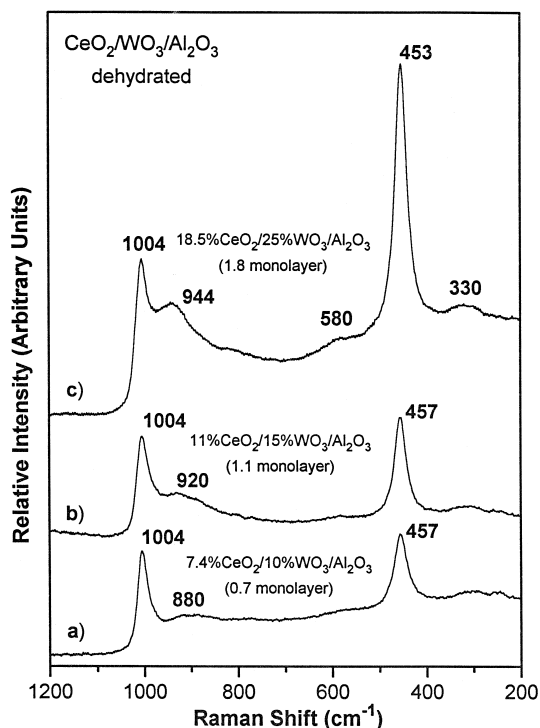


Fig. 8. (a) 7.4% CeO₂/10% WO₃/Al₂O₃ (0.7 monolayer), (b) 11% CeO₂/15% WO₃/Al₂O₃ (1.1 monolayer) and (c) 18.5% CeO₂/25% WO₃/Al₂O₃ (1.8 monolayer).

oxide species (centered at 964 cm⁻¹) is very broad in the hydrated spectrum and overshadows any weak features around 944 cm⁻¹ [28]. In summary, all of these observations represent very minor changes to the Raman spectra of the catalysts promoted by P₂O₅, SnO₂, Fe₂O₃, NiO, ZnO, CoO, CeO₂ and MgO, relative to unpromoted WO₃/Al₂O₃, so these secondary metal oxide additives are considered essentially noninteracting.

The interacting secondary metal oxide additives include La₂O₃, CaO, K₂O and Na₂O (Figs. 9, 10, 12 and 13, respectively). Catalysts containing these secondary metal oxides have Raman spectra which significantly differ from those of unpromoted WO₃/Al₂O₃ in two ways. First, all of these additives lower the frequency of the W=O symmetric stretch by substantial amounts (~33–55 cm⁻¹ at the highest loading of 1.8 monolayer-equivalents), corresponding to

an increase in the W=O bond length [13,16]. Second, the most strongly interacting additives form crystalline compounds with the tungsten oxide, as indicated by identical hydrated and dehydrated spectra (unlike surface species, which readily hydrate and change their Raman features, most crystal vibrations are unaffected by the presence of water [24]). While the downshift of the W=O band by these specific interacting additives occurs at both low and high loadings, compound formation is restricted mainly to loadings above 1 monolayer-equivalent.

For example, strong interaction between surface tungsten oxide species with surface species of Na₂O and K₂O is evidenced by much lower frequencies of the W=O symmetric stretch relative to the frequencies of this mode in the unpromoted WO₃/Al₂O₃ catalysts. In samples promoted by Na₂O, this band shifts down to

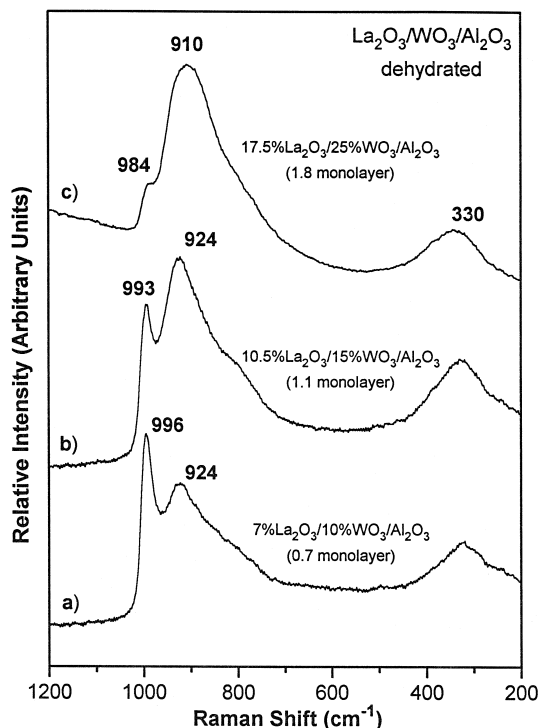


Fig. 9. (a) 7% La₂O₃/10% WO₃/Al₂O₃ (0.7 monolayer), (b) 10.5% La₂O₃/15% WO₃/Al₂O₃ (1.1 monolayer) and (c) 17.5% La₂O₃/25% WO₃/Al₂O₃ (1.8 monolayer).

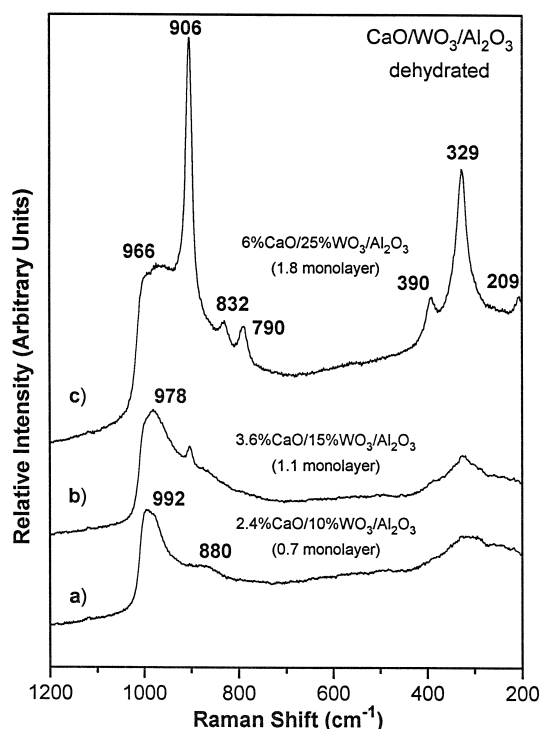


Fig. 10. (a) 2.5% CaO/10% WO₃/Al₂O₃ (0.7 monolayer), (b) 3.6% CaO/15% WO₃/Al₂O₃ (1.1 monolayer) and (c) 6% CaO/25% WO₃/Al₂O₃ (1.8 monolayer).

991, 974 and 966 cm⁻¹ as loading is increased, while in K₂O-promoted samples the frequency shifts to 978, 978 and 962 cm⁻¹. For the highest loading, this corresponds to a downshift in the W=O band of 51 and 55 cm⁻¹ for catalysts promoted by Na₂O and K₂O, respectively. The similar hydrated [28] and dehydrated spectra of catalysts promoted by K₂O and Na₂O at the highest loading (1.8 monolayer-equivalents) suggest the possibility of crystalline compound formation, but the close agreement in band positions and shapes of the ~880, ~580 and ~235 cm⁻¹ polymeric bands with these same bands in unpromoted WO₃/Al₂O₃ suggests that surface tungsten oxide species are present on these catalysts, not crystalline compounds. Also, the spectra of known alkali tungstates [36,37] do not match the spectra of the catalysts promoted by K₂O and Na₂O. Nevertheless, strong interaction with surface tungsten oxide is clearly indi-

cated for the secondary metal oxide additives Na₂O and K₂O.

For CaO-promoted catalysts, the interaction with tungsten oxide appears to be even stronger. The W=O band is downshifted by CaO from 1004 to 992 cm⁻¹ for the lowest loading and from 1017 to 966 cm⁻¹ for the highest loading. In addition, for the 6% CaO/25% WO₃/Al₂O₃ catalyst, the sharp, well-defined peaks at 909, 833, 793, 387, 326 and 206 cm⁻¹ are characteristic of crystalline CaWO₄ [13,38], and these same crystalline bands appear in the hydrated spectrum [28]. Note that the W=O band of the tungsten oxide surface species does not overlap with the bands of the CaWO₄ compound, and hence the surface species and crystalline compounds can be distinguished.

Similarly, the samples promoted with La₂O₃ have strong bands at ~910 and ~330 cm⁻¹ that also appear in the hydrated spectra [28],

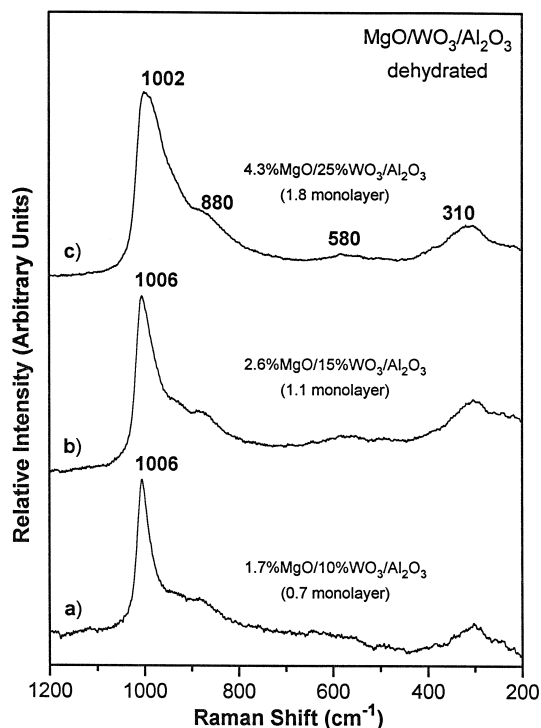


Fig. 11. (a) 1.7% MgO/10% WO₃/Al₂O₃ (0.7 monolayer), (b) 2.6% MgO/15% WO₃/Al₂O₃ (1.1 monolayer) and (c) 4.3% MgO/25% WO₃/Al₂O₃ (1.8 monolayer).

indicating compound formation. The weak W–O–W bands of the tungsten oxide surface species at ~ 580 and 210 cm^{-1} are also absent. While the bands at 910 and 330 cm^{-1} in the $\text{La}_2\text{O}_3/\text{WO}_3/\text{Al}_2\text{O}_3$ catalysts are somewhat consistent with the bands of $\text{La}_2(\text{WO}_4)_3$ at 945 , 926 , 726 , 383 and 335 cm^{-1} [35], the broadness of the bands prevents definitive identification. The slightly different Raman band positions are most likely due to small or poorly crystallized $\text{La}_2(\text{WO}_4)_3$ particles. As with CaO-promoted samples, the W=O band of the tungsten oxide surface species does not overlap with the bands of the lanthanum compound and can be seen to exist even at the highest loading. However, this surface tungsten oxide species is highly influenced by the lanthanum oxide, since the stretching frequency of the terminal W=O band in the tungsten oxide surface species shifts down to

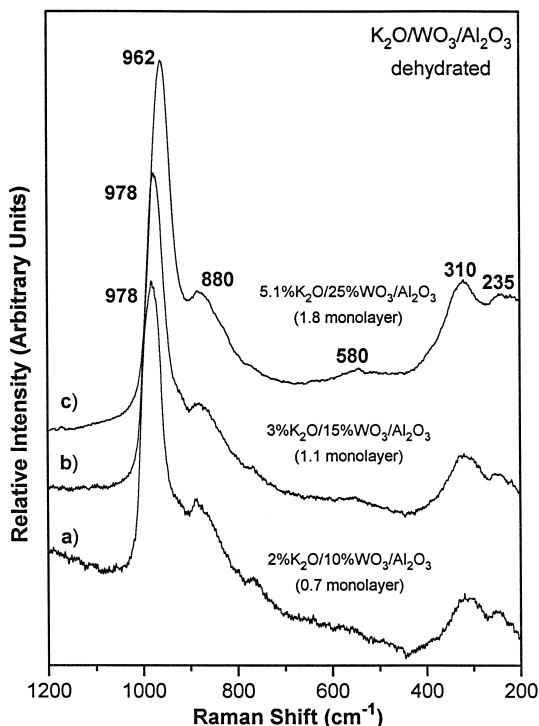


Fig. 12. (a) 2% $\text{K}_2\text{O}/10\% \text{WO}_3/\text{Al}_2\text{O}_3$ (0.7 monolayer), (b) 3% $\text{K}_2\text{O}/15\% \text{WO}_3/\text{Al}_2\text{O}_3$ (1.1 monolayer) and (c) 5% $\text{K}_2\text{O}/25\% \text{WO}_3/\text{Al}_2\text{O}_3$ (1.8 monolayer).

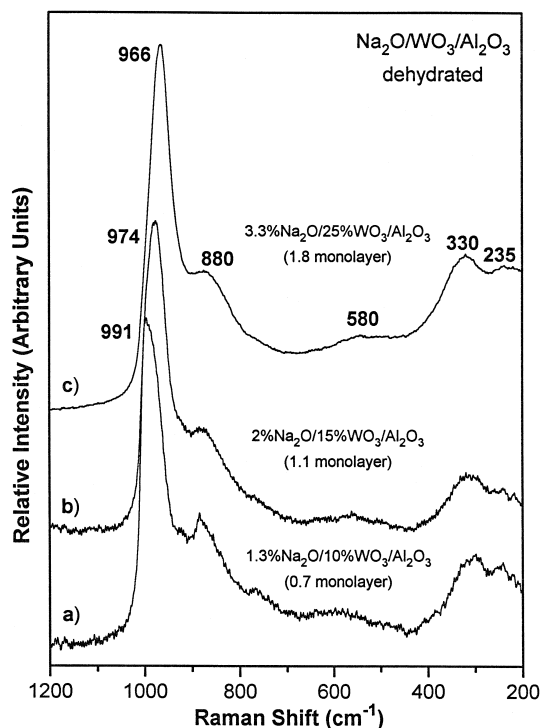


Fig. 13. (a) 1.3% $\text{Na}_2\text{O}/10\% \text{WO}_3/\text{Al}_2\text{O}_3$ (0.7 monolayer), (b) 2% $\text{Na}_2\text{O}/15\% \text{WO}_3/\text{Al}_2\text{O}_3$ (1.1 monolayer) and (c) 3.3% $\text{Na}_2\text{O}/25\% \text{WO}_3/\text{Al}_2\text{O}_3$ (1.8 monolayer).

996 and 984 cm^{-1} at low and high loadings, respectively.

4. Discussion

4.1. $\text{WO}_3/\text{Al}_2\text{O}_3$ catalysts

A full discussion of the unpromoted $\text{WO}_3/\text{Al}_2\text{O}_3$ catalyst under dehydration was presented by Vuurman et al. [23] and only a brief summary is given here. The major Raman band at $\sim 1000\text{--}1020\text{ cm}^{-1}$, assigned to the terminal W=O bond in the tungsten oxide surface species, was shown to be present as a single, mono-oxo (W=O) species rather than as a di-oxo (O=W=O) species [23,39–44]. Also, the coordination of the dehydrated surface tungsten oxide species was found by in situ XANES

[13] to be a function of surface coverage. The surface tungsten oxide was found to exist as tetrahedrally coordinated monomers at low coverages ($< 1/3$ monolayer) and as a mixture of tetrahedrally and octahedrally coordinated surface polymers at high loadings. This observation is confirmed in the current study by an increase in the relative intensity of the Raman bands at ~ 580 and $\sim 210 \text{ cm}^{-1}$, which have been assigned to W–O–W polymeric linkages [23], with increasing tungsten oxide loading (see Fig. 1).

Similar results were recently found for the alumina supported molybdenum oxide system from in situ Raman and XANES studies: isolated, tetrahedrally coordinated surface molybdenum oxide species were present at low surface coverage and a polymerized mixture of octahedrally/tetrahedrally coordinated surface molybdenum oxide species were present at monolayer coverage [45,46]. The supported molybdenum oxide in situ XANES measurements also revealed that the molecular structure of the surface metal oxide species can vary with the specific oxide support and, consequently, in situ XANES measurements for WO_3/TiO_2 catalysts cannot be extrapolated to in situ XANES measurements for $\text{WO}_3/\text{Al}_2\text{O}_3$ catalysts, which Hilbrig et al. assumed [46].

4.2. Noninteracting metal oxide additives

Noninteracting metal oxide additives are defined as those additives that do not significantly perturb the Raman vibrations of the surface tungsten oxide species and preferentially interact with the alumina support. The metal oxide additives P_2O_5 , SnO_2 , Fe_2O_3 , NiO , ZnO , CoO , CeO_2 and MgO fall into this category because they did not significantly perturb the W=O and W–O–W Raman vibrations of the surface tungsten oxide species. However, this result is in conflict with those of Schwarz et al. [47–49], whose group has proposed the existence of Ni–W [48] and Co–W [49] interaction species

on the basis of temperature programmed reduction, X-ray diffraction and oxidation activity studies. In the present investigation, neither NiWO_4 crystals or $\text{Co}_2\text{W}_{12}\text{O}_{42}^{-8}$ heteropolytungstate ions, the suggested interaction species, were detected in the dehydrated Raman spectra. While there is some possibility of heteropolytungstate formation in the hydrated catalysts [28], the only evidence detected in the dehydrated Raman data for Ni–W or Co–W interaction is a slight enhancement, relative to unpromoted $\text{WO}_3/\text{Al}_2\text{O}_3$, of the broad band due to O–W–O symmetric stretching at $\sim 880 \text{ cm}^{-1}$. In general, however, the dehydrated Raman spectra of these Ni- and Co-promoted catalysts appear very similar to unpromoted $\text{WO}_3/\text{Al}_2\text{O}_3$, especially regarding the frequency of the W=O symmetric stretch, and, therefore, do not support the presence of significant Ni–W or Co–W interaction.

Surprisingly, the alumina support was able to simultaneously accommodate approximately a monolayer of each of the above metal oxide additives in the presence of a monolayer of surface tungsten oxide species without the formation of crystalline metal oxide phases. Only trace crystalline particles of WO_3 were observed in the presence of P_2O_5 (at 1.8 monolayer-equivalents coverage) and in the presence of Fe_2O_3 , while trace CeO_2 particles were detected in the presence of ceria. The ability of the alumina support to accommodate such high loadings of two surface metal oxides suggests that the two metal oxide species are occupying different locations or sites on the alumina surface. The surface tungsten oxide species anchor to the alumina support by titrating the surface hydroxyls of the alumina surface [50,51] and oxides such as Fe, Ni, Zn and Co preferentially interact with the coordinately unsaturated Al^{+3} Lewis acid surface sites [44]. P_2O_5 reacts with the alumina surface to make a surface compound [52]. Not much is currently known about the location of the surface tin oxide species on alumina. The noninteracting additives fall into the category of oxides that are acidic or mildly

basic as measured by their net pH at pzc [28], although CeO_2 and MgO are somewhat exceptional because they are quite basic but have little interaction with the surface tungsten oxide species.

4.3. Interacting metal oxide additives

Interacting metal oxide additives are defined as those metal oxide additives that significantly perturb the Raman vibrations of the surface tungsten oxide species by preferentially interacting with the surface tungsten oxide species (formation of a surface mixed metal oxide complex) or a crystalline mixed tungsten oxide compound. The metal oxide additives that fall into this category are La_2O_3 , CaO , K_2O and Na_2O since they significantly perturb the surface tungsten oxide species or form crystalline mixed tungsten oxide compounds.

At lower surface coverage (0.7 monolayer-equivalent), the above metal oxide additives primarily interacted with the surface tungsten oxide species to form surface mixed metal oxide complexes that shifted the Raman band of the terminal $\text{W}=\text{O}$ bond to lower wavenumbers. This shift reflects an increase in the $\text{W}=\text{O}$ bond length due to less distortion of the surface tungsten oxide species in the presence of these secondary metal oxides. Furthermore, it reveals that these secondary metal oxide additives are directly interacting with the surface tungsten oxide species. At higher surface coverage (1.8 monolayer-equivalents), the downshift in the Raman frequency of the $\text{W}=\text{O}$ bond increases and, in addition, a reaction of La_2O_3 and CaO with the surface tungsten oxide species forms crystalline mixed tungsten oxide compounds. However, even additives forming crystalline compounds also have bands characteristic of the symmetric stretch of the terminal $\text{W}=\text{O}$ bond in tungsten oxide surface species, indicating that these surface tungsten oxide species coexist with the crystalline compounds at high loadings. The interacting additives fall into the category of

metal oxides that are basic as measured by their net pH at pzc [28].

4.4. Differences between hydrated and dehydrated catalysts

It was found for the hydrated catalysts that the tungsten oxide surface species present on the catalysts were determined by the net pH at the point of zero charge (pzc) of the thin aqueous film on the catalyst surface [28]. The secondary metal oxides influenced the molecular structures of the tungsten oxide surface species indirectly by changing the net pH at pzc of this thin aqueous film. No direct interaction between the tungsten oxide and the secondary metal oxides was detected in the hydrated catalysts due to the hydrolyzing effect of the aqueous medium, which separates the metal oxide species into ions. Instead, only indirect interaction between the ions was allowed, by charge transfer through the water, as measured by the net pH at pzc. Contescu et al. [47] have also identified the importance of water as a charge transfer medium for the interaction of tungsten oxide species with protonated alumina hydroxyls, the interaction which they attribute to the formation of polytungstate ions on the surface of hydrated $\text{WO}_3/\text{Al}_2\text{O}_3$.

For dehydrated catalysts, however, changes in the Raman spectra are interpreted as an indication of direct chemical interaction between the tungsten oxide and the secondary metal oxide surface species, since the alumina surface is a much poorer charge transfer medium than the homogeneous, liquid-phase aqueous thin film present during hydrated conditions. For this reason, different metal oxide species, anchored to different alumina surface sites, can only interact with each other by direct contact when a charge transfer medium, like water, is absent. For example, both CeO_2 and MgO have the ability to influence the structure of the solvated surface tungsten oxide species by raising the net pH at pzc of the thin aqueous film which is present under ambient conditions [28], but they have

very little influence on the structures of surface tungsten oxide species under dehydrated conditions (where direct contact is required for interaction). Hence, for dehydrated catalysts a clear grouping of the secondary metal oxides can be made, based on changes in the Raman spectra relative to the unpromoted $\text{WO}_3/\text{Al}_2\text{O}_3$ catalysts, into those that directly interact with tungsten oxide surface species and those that do not.

5. Conclusion

The dehydrated Raman spectra of unpromoted $\text{WO}_3/\text{Al}_2\text{O}_3$ indicate that these tungsten oxide surface species have the mono-oxo structure, and are present as tetrahedrally coordinated monomers at low loadings and as a mixture of tetrahedrally and octahedrally coordinated surface polymers at high loadings. The effect of additives on the dehydrated structure of the surface tungsten oxide species in $\text{WO}_3/\text{Al}_2\text{O}_3$ catalysts is generally described as either noninteracting or interacting, based on the effect that a specific additive has on the Raman spectrum of the surface tungsten oxide species. Noninteracting additives, including P_2O_5 , SnO_2 , Fe_2O_3 , NiO , ZnO , CoO , CeO_2 and MgO do not significantly affect the structure of the surface tungsten oxide phase because they coordinate directly to the alumina support on sites different from those of the tungsten oxide surface species (which anchor to the alumina hydroxyls). Interacting additives, including La_2O_3 , CaO , K_2O and Na_2O , however, have a pronounced effect on the structure of the surface tungsten oxide phase. The interacting additives form both surface mixed metal oxide species and, for La_2O_3 and CaO , crystalline tungsten oxide compounds with the surface tungsten oxide species. These interacting additives tend to be rather basic (La_2O_3 , CaO , K_2O and Na_2O), as measured by the net pH at pzc of their hydrated surfaces. The noninteracting additives tend to be acidic (P_2O_5 and SnO_2) or mildly basic (Fe_2O_3 , NiO , ZnO , CoO , CeO_2 and MgO).

Acknowledgements

This work was gratefully supported by the U.S. Department of Energy under grant #DEFG02-93ER14350.

References

- [1] C.L. Thomas, *Catalytic Processes and Proven Catalysts*, Academic Press, New York, 1970.
- [2] L.L. Murrell, C.J. Kim, D.C. Grenoble, U.S. Pat. No. 4,233,139, 1980.
- [3] D.C. Grenoble, C.J. Kim, L.L. Murrell, U.S. Pat. No. 4,440,872, 1984.
- [4] J. Bernholc, J.A. Horsley, L.L. Murrell, L.G. Sherman, S. Soled, *J. Phys. Chem.* 91 (1987) 1526.
- [5] L.L. Murrell, D.C. Grenoble, C.J. Kim, N.C. Dispenziere, *J. Catal.* 107 (1987) 463.
- [6] C. Wivel, B.S. Clausen, R. Candia, S. Morup, H. Topsøe, *J. Catal.* 87 (1984) 497.
- [7] H. Knozinger, *Proc. 9th Int. Congr. Catalysis*, vol. 5, 1988, p. 20.
- [8] F.T. Clark, A.L. Hensley, J.Z. Shyu, J.A. Kaduk, G.J. Ray in: J.B. Butt, C.H. Bartholomew (Eds.), *Catalyst Deactivation 1991*, vol. 68, Elsevier Science Publishers, Amsterdam, 1991, p. 417.
- [9] F.T. Clark, A.L. Hensley, U.S. Pat. No. 4,994,423, 1991.
- [10] F.T. Clark, A.L. Hensley, U.S. Pat. No. 4,997,799, 1991.
- [11] F.T. Clark, A.L. Hensley, U.S. Pat. No. 5,071,538, 1991.
- [12] D.S. Kim, M.M. Ostromecki, I.E. Wachs, *J. Mol. Catal. A* 106 (1996) 93.
- [13] J.A. Horsley, I.E. Wachs, J.M. Brown, G.H. Via, F.D. Hardcastle, *J. Phys. Chem.* 91 (1987) 4014.
- [14] S.S. Chan, I.E. Wachs, L.L. Murrell, *J. Catal.* 90 (1984) 150.
- [15] S.S. Chan, I.E. Wachs, L.L. Murrell, N.C. Dispenziere Jr., *J. Catal.* 92 (1985) 1.
- [16] F.D. Hardcastle, I.E. Wachs, *J. Raman Spectrosc.* 26 (1995) 397.
- [17] I.E. Wachs, C.C. Chersich, J.H. Hardenbergh, *Appl. Catal.* 13 (1985) 335.
- [18] J.C. Carver, I.E. Wachs, L.L. Murrell, *J. Catal.* 100 (1986) 500.
- [19] P. Biloen, G.T. Pott, *J. Catal.* 30 (1973) 169.
- [20] D.C. Vermaire, P.C. van Berge, *J. Catal.* 116 (1989) 309.
- [21] S.L. Soled, G.B. McVicker, L.L. Murrell, L.G. Sherman, N.C. Dispenziere Jr., S.L. Hsu, D. Waldman, *J. Catal.* 111 (1988) 286.
- [22] R.L. Brady, D. Southmayd, C. Contescu, R. Zhang, J.A. Schwarz, *J. Catal.* 129 (1991) 195.
- [23] M.A. Vuurman, I.E. Wachs, *J. Phys. Chem.* 96 (1992) 5008.
- [24] I.E. Wachs, F.D. Hardcastle, S.S. Chan, *Spectroscopy* 1 (1986) 30.
- [25] F.D. Hardcastle, I.E. Wachs, *Catalysis*, vol. 10, Royal Society of Chemistry, Cambridge, UK, 1993, pp. 102–153.
- [26] J.M. Stencel, *Raman Spectroscopy for Catalysis*, Van Nostrand Reinhold, New York, 1990.

- [27] G. Deo, I.E. Wachs, *J. Phys. Chem.* 95 (1991) 5889.
- [28] M.M. Ostromecki, L.J. Burcham, I.E. Wachs, N. Ramani, J.G. Ekerdt, *J. Mol. Catal. A* 132 (1998) 43.
- [29] J.M. Stencel, L.E. Makovsky, J.R. Diehl, T.A. Sarkus, *J. Catal.* 95 (1985) 414.
- [30] E. Payen, M.C. Dhamelinourt, P. Dhamelinourt, J. Grimblot, J.P. Bonnelle, *Appl. Spectrosc.* 36 (1982) 30.
- [31] M.A. Vuurman, I.E. Wachs, A.M. Hirt, *J. Phys. Chem.* 95 (1991) 9928.
- [32] M.A. Vuurman, I.E. Wachs, *J. Mol. Catal.* 77 (1992) 29.
- [33] S.S. Chan, I.E. Wachs, *J. Catal.* 103 (1987) 224.
- [34] J.Z. Shyu, W.H. Weber, H.S. Gandhi, *J. Phys. Chem.* 92 (1988) 4964.
- [35] L.J. Burcham, I.E. Wachs, *Spectrochim. Acta A* (1997), submitted.
- [36] H.J. Becher, *J. Less-Common Metals* 76 (1980) 169.
- [37] F. Knee, R.A. Condrate Sr., *J. Phys. Chem. Solids* 40 (1979) 1145.
- [38] J.P. Russell, R. Loudon, *Proc. Phys. Soc.* 85 (1965) 1029.
- [39] L. Wang, Ph.D. thesis, The University of Wisconsin, Milwaukee, 1982.
- [40] G. Ramis, G. Busca, C. Cristiani, L. Lietti, P. Forzatti, F. Bregani, *Langmuir* 8 (1992) 1744.
- [41] B. Soptrajanov, A. Nikolovski, I. Petrov, *Spectrochim. Acta A* 24 (1968) 1617.
- [42] W. Levason, R. Narayanaswamy, R. Ogden, J.S. Rest, A.J. Turff, *J. Chem. Soc. Dalton Trans.* (1982) 2009.
- [43] D.S. Kim, I.E. Wachs, K. Segawa, *J. Catal.* 146 (1994) 268.
- [44] M.A. Vuurman, Ph.D. thesis, University of Amsterdam, 1992.
- [45] H. Hu, I.E. Wachs, S.R. Bare, *J. Phys. Chem.* 99 (1995) 10897.
- [46] F. Hilbrig, H.E. Gobel, H. Knozinger, H. Schmelz, B. Lengeler, *J. Phys. Chem.* 95 (1991) 6973.
- [47] C. Contescu, J. Jagiello, J.A. Schwarz, *J. Phys. Chem.* 97 (1993) 10152.
- [48] D.W. Southmayd, C. Contescu, J.A. Schwarz, *J. Chem. Soc. Faraday Trans.* 89 (1993) 2075.
- [49] R. Zhang, J.A. Schwarz, A. Datye, J. P Baltrus, *J. Catal.* 135 (1992) 200.
- [50] A.M. Turek, I.E. Wachs, E.C. Decanio, *J. Phys. Chem.* 96 (1992) 5000.
- [51] M.A. Vuurman, I.E. Wachs, D.J. Stufkens, A. Oskam, *J. Mol. Catal.* 80 (1993) 209.
- [52] J. Shen, R.D. Cortright, Y. Chen, J.A. Dumesic, *J. Phys. Chem.* 98 (1994) 8067.